Scaling and vortex-string dynamics in a three-dimensional system with a continuous symmetry

M. Mondello and Nigel Goldenfeld

*Department of Physics and Materials Research Laboratory,
University of Illinois at Urbana-Champaign, 1110 West Green Street, Urbana, Illinois 61801*
(Received 22 July 1991)

We study the dynamics of a three-dimensional system with a nonconserved complex order parameter $\Psi(\mathbf{r},t)$, following a quench below the ordering transition temperature. For a critical quench [$\langle \Psi(\mathbf{r},0) \rangle = 0$] we observe dynamical scaling and an effective value of the dynamical exponent of $\phi = 0.45 \pm 0.01$. For an off-critical quench [$\langle \Psi(\mathbf{r},0) \rangle \neq 0$] there is a breakdown of dynamical scaling and the vortex-string length $l(t)$ varies with time t as $l(t) \sim t^{-1} \exp(-\gamma t^{3/2})$, in good agreement with a theoretical calculation by Toyoki and Honda. The predicted relation $\gamma \propto |\langle \Psi(\mathbf{r},0) \rangle|^2$ is found to represent only a lower bound. We indicate the possible relevance of these results for liquid-crystal systems and cosmological pattern formation.

PACS number(s): 64.60.Ht, 67.40.Vs, 64.60.Cn, 98.80.Cq

I. INTRODUCTION

Scaling phenomena are often observed during the approach to equilibrium [1]. The classic example is spinodal decomposition of a binary alloy, where the system proceeds to its final state of two-phase coexistence through the development of a pattern characterized by a single time-dependent length scale λ. It has been found that λ varies with time t according to $\lambda(t) \sim t^{\phi}$, where the dynamical exponent $\phi = \frac{1}{3}$ for the case of a conserved order parameter and $\phi = \frac{1}{2}$ for the case of a nonconserved order parameter [2,3]. These results do not seem to depend upon the dimension D of the system, above its lower critical dimension. Furthermore, the order-parameter dynamical scattering function is found to obey a scaling law

$$S(k,t) = [\lambda(t)]^D \Phi(k\lambda(t)) , \qquad (1.1)$$

where $\Phi(x)$ is referred to as a scaling function. Considerable analytical and numerical work has recently been devoted to the study of the relaxation dynamics in systems with a continuous symmetry [4–8]. In a previous paper [5] we investigated the relaxation dynamics of a two-dimensional system with a nonconserved complex order parameter, in order to address the issue of the effect of the continuous symmetry of the order parameter and the associated topological defects (vortices) on the relaxation process. We found that at late times $\phi = 0.50 \pm 0.02$, and we observed dynamical scaling not only for the order-parameter scattering function but also for the real-space vortex-vortex correlation functions. We have since extended our investigation, introducing a vector gauge field in our model to consider the case of the ordering dynamics of a charged system (superconductor) [6].

The purpose of the present paper is to study a three-dimensional neutral system with complex order parameter, where a vortex-string network of total length $l(t)$ develops after the quench. This system has been investigated theoretically by Toyoki and Honda [9], using the

defect-dynamics picture of the relaxation process proposed by Kawasaki [10]. In this picture the relaxation is driven by the long-range current-current interaction among the strings, analogous to the Biot-Savart law of classical electromagnetism. In their study, Toyoki and Honda made the further simplifying assumption that the strings are driven only by the tension associated with their local curvature and that string crossing and reconnection may be ignored. This corresponds to a mean-field level description of the system. Technically the strings are described in terms of the intersection of two surfaces representing the zeros of two auxiliary scalar fields, which obey simple diffusive dynamics [11].

In our simulations we identify the two auxiliary scalar fields with the two components of the complex order parameter. With this identification, the predictions of Toyoki and Honda [9] are such that in the case of a critical quench [spatial average $\langle \Psi(\mathbf{r},0) \rangle = 0$], there will be dynamical scaling in the intermediate asymptotic behavior of the system (after possible transients and before finite-size effects set in), and an effective exponent of $\phi = \frac{1}{2}$ is predicted for the time dependence of the characteristic length scale λ of the system. For a system of linear dimension L, we can choose $\lambda(t)$ to be average intervortex spacing $\sqrt{L^3/l(t)}$ (see Sec. III) so that $l(t) \sim t^{-2\phi}$. In the case of an off-critical quench [$\langle \Psi(\mathbf{r},0) \rangle \neq 0$], there is predicted to be a systematic deviation from scaling and a much faster decay of the total vortex-string length:

$$l(t) \sim t^{-1} \exp(-\gamma t^{3/2}) , \qquad (1.2)$$

where $\gamma \propto |\langle \Psi(\mathbf{r},0) \rangle|^2$, so that we recover the critical-quench result in the limit $|\langle \Psi(\mathbf{r},0) \rangle| \to 0$. This exponential decay is due to an early breakup of the string network and successive independent shrinking of the remnant loops. The dynamics of the breakup, of course, cannot be treated in mean-field theory, but, as we show below (see Sec. V), the asymptotic time dependence of the vortex-string decay is controlled by the loop-size distribution after the breakup, and this distribution is implicitly in-

corporated in the initial conditions for the auxiliary fields.

The results of our simulations are in good qualitative and semiquantitative agreement with these theoretical predictions and strongly support the physical picture of the relaxation process on which they are based. In particular, for a critical quench, we find evidence of dynamical scaling and an effective value of the dynamical exponent of $\phi=0.45\pm0.01$, so that $l(t)\sim t^{-0.90\pm0.02}$. This should be contrasted with a previous numerical study by Nishimori and Nukii [7], who found that the length of the defect line decreases with time as $l(t)\sim t^{-0.75\pm0.05}$. It is likely that their simulations were not in the true asymptotic regime because of the relatively small size of the system considered [12]. In the case of an off-critical quench, we see the emergence of two dynamically generated length scales: the average size of vortex loops, which has only a weak time dependence, and the average interloop spacing, which increases exponentially with time. This leads to a breakdown of the dynamical scale invariance and an exponential decay of $l(t)$ consistent with the predictions of Toyoki and Honda [9]. The relation $\gamma \propto |\langle \Psi(r,0)\rangle|^2$ is at least qualitatively satisfied, and appears to represent a lower bound to the observed functional dependence.

An experimental study of the coarsening dynamics of a bulk nematic liquid crystal has recently been reported by Chuang, Turok, and Yurke [13]. They find that the evolution of the density of strings with topological charge $\pm\frac{1}{2}$, $\rho_s(t)$, is consistent with simple scaling and agrees with the mean-field prediction $\rho_s\sim t^{-1}$. One way of testing experimentally the results of our simulations for the off-critical quench would be to repeat the experiment of Chuang, Turok, and Yurke [13] performing the temperature (or pressure) quenches in the presence of a magnetic field or other appropriately chosen bias. In order to preserve the conditions of our numerical simulation, the field should be switched off immediately after the quench, before late-stage coarsening sets in; it would be interesting to consider also the case of a time-independent external field.

For the case of a system whose order parameter is a scalar (i.e., with a discrete symmetry), there are already experiments that investigate the role of bias on the coarsening dynamics of twisted nematic liquid crystals, following a quench below the clearing-point temperature [14,15]. In these experiments the bias is introduced by certain boundary conditions (anchoring at rubbed walls) that control the twisting of the order parameter across the system, with two degenerate states (below the transition temperature) and $\frac{1}{2}$-disclination lines [16] separating the corresponding domains, while the nonorthogonal twisting is equivalent to the introduction of an external field favoring one state with respect to the other. Ordinary dynamical scaling with a dynamical exponent $\phi=\frac{1}{2}$ was found in the unbiased case [14], but the introduction of nonorthogonal twisting led to a breakdown of simple (single-length) scaling and much faster relaxation [15], which the authors did not try to quantify. Again, a closer experimental realization of the conditions of our simulations and of earlier simulations of Toyoki and

Honda [17], which directly apply to the scalar case, would require a rearrangement of the boundary conditions (from nonorthogonal to orthogonal) immediately following the quench. In any case, we believe that the more significant effect of the "external field" is on the initial conditions rather than on the coarsening process itself [18]. We expect, therefore, that the principal features of the ordering dynamics in the presence of biased initial conditions will occur, at least qualitatively, even when the bias is provided by a time-independent external field.

In Sec. II we introduce our model and describe some of the qualitative features of the dynamics. Section III is devoted to a quantitative analysis of the relaxation dynamics in terms of a typical time-dependent length scale. In this section we compare five possible choices for the characteristic length scale and discuss the results for the power-law exponent ϕ. In Sec. IV we consider the dynamical scaling behavior of real-space and momentum-space correlation functions following a critical quench. The off-critical-quench case is discussed in Sec. V. We summarize our conclusions and make a few final remarks in Sec. VI.

During the drafting of this paper we learned of related work by Toyoki [8]. He also reports the results of a numerical study of the relaxation dynamics of a complex nonconserved order parameter on a 64^3 lattice, using a discretization scheme similar to ours. For the critical-quench case, the only case considered in his paper, he also finds a dynamical exponent $\phi=0.45\pm0.01$. The fact that his result does not show any statistically significant difference with ours, obtained using a larger (128^3) lattice, seems to indicate that systematic finite-size corrections are not dominant [19], which of course does not exclude the possibility that, in the time range considered, we are observing a transient state of our system.

II. MODEL

We consider a complex nonconserved order-parameter field on a $L \times L \times L$ lattice in three dimensions. This may be considered to be a caricature of the superfluid transition or of the ferromagnetic transition of a planar ferromagnet in three dimensions. The evolution of the order-parameter field $\Psi(r,t)\equiv X(r,t)+iY(r,t)$ is governed by a phenomenological equation similar to that of a system with a discrete symmetry:

$$\frac{\partial\Psi(r,t)}{\partial t}=-M\frac{\partial F(\Psi(r,t))}{\partial\Psi^*(r,t)} , \qquad (2.1)$$

where M is a kinetic coefficient, assumed to be independent of Ψ and

$$F(\Psi(r,t))=\int d^2r \left[|\nabla\Psi(r,t)|^2-a|\Psi(r,t)|^2 \right. \\ \left. +\frac{b}{2}|\Psi(r,t)|^4 \right] . \qquad (2.2)$$

The coefficients a and b are positive after the quench. We performed our simulations using a cell-dynamics scheme, a computationally efficient coarse grained description of

the ordering dynamics [20]. The evolution of the system is controlled, in our case, by the local (on-site) nonlinear relaxation process and isotropic Laplacian averaging, which couples nearest-neighbor (NN) and next-nearest-neighbor (NNN) sites. The corresponding equations in terms of the $X(\mathbf{r},t)$ and $Y(\mathbf{r},t)$ fields read

$$X(\mathbf{n},t+1)= A\tanh[R(\mathbf{n},t)][X(\mathbf{n},t)/R(\mathbf{n},t)]$$
$$+C[\langle\langle X(\mathbf{n},t)\rangle\rangle-X(\mathbf{n},t)]\ ,$$
$$Y(\mathbf{n},t+1)= A\tanh[R(\mathbf{n},t)][Y(\mathbf{n},t)/R(\mathbf{n},t)] \quad (2.3)$$
$$+C[\langle\langle Y(\mathbf{n},t)\rangle\rangle-Y(\mathbf{n},t)]\ ,$$

where $R(\mathbf{n},t)=|\Psi(\mathbf{n},t)|$ and

$$\langle\langle\psi(n,t)\rangle\rangle \equiv \sum_{\langle\mathrm{NN}\rangle}\left[\frac{\psi(\mathbf{m},t)}{9}\right]+\sum_{\langle\mathrm{NNN}\rangle}\left[\frac{\psi(\mathbf{m},t)}{36}\right]\ . $$
$$(2.4)$$

Here $\mathbf{n}$ and $\mathbf{m}$ represent the lattice sites, A gives a mea-

sure of the depth of the quench, and C controls the coupling strength. The unit of time is implicitly defined in terms of A and C. For our simulations we choose $A=1.3$ and $C=0.5$. These parameters describe the system after the quench ($A>1$), when the initial high-temperature configuration of the order-parameter field becomes unstable.

For the critical-quench case, the initial values of the vector components of Ψ are randomly chosen to be between -0.1 and 0.1 of their final equilibrium length (~ 1). Thus, initially ($t=0$) the relative orientations of the vectors are random (uncorrelated) and the spatial average $\langle\Psi(\mathbf{r},0)\rangle=0$ [21]. As order develops in our system, the order-parameter field Ψ grows in modulus, and sensitive only to its local environment, it reorients itself, choosing one of its new (infinitely degenerate) equilibrium configurations. The ensuing mismatch at the boundaries of growing ordered domains leads to the formation of a defect network. The topologically stable defects in our system are vortex strings characterized by an integer winding number n. Strings with $|n|>1$ are (energetically) unstable towards the formation of strings with $|n|=1$, so that $|n|=1$ vortex strings are the only ones relevant to the asymptotic dynamics of the system. We can, therefore, describe the system relaxation in terms of the gradu-
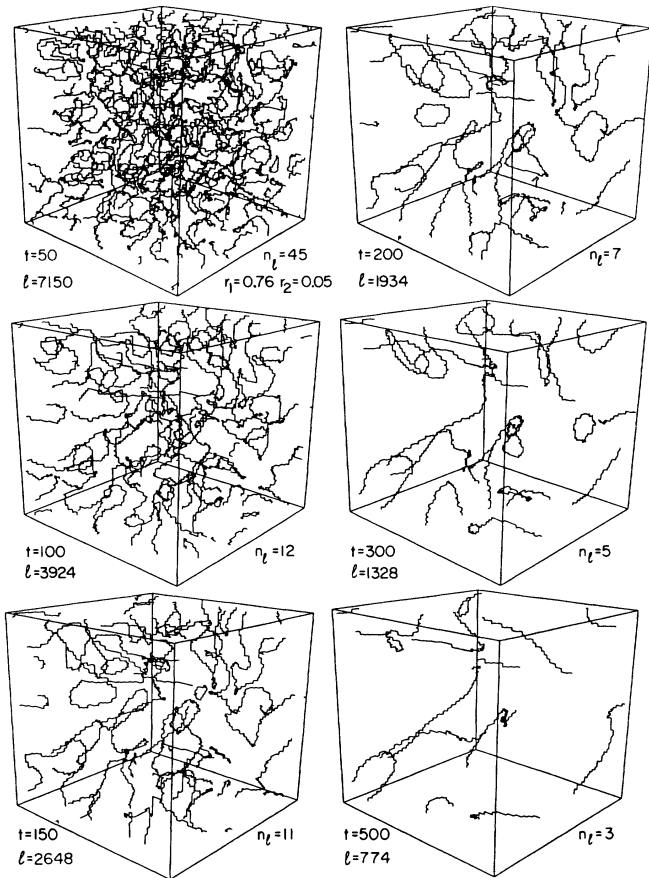

FIG. 1. Evolution of the string network after a critical quench at $t=0$. Below each "snapshot" of the system we give the total string length [$l(t)$] and the number of independent loops present [$n_l(t)$]. To characterize the loop-size distribution at early times we give $r_n\equiv l_n(t)/l(t)$, where $l_n(t)$ is the length of the nth largest loop. For illustration purposes here we use a 64^3 lattice, while all the numerical data used in the statistical averages were collected on 128^3 lattices.
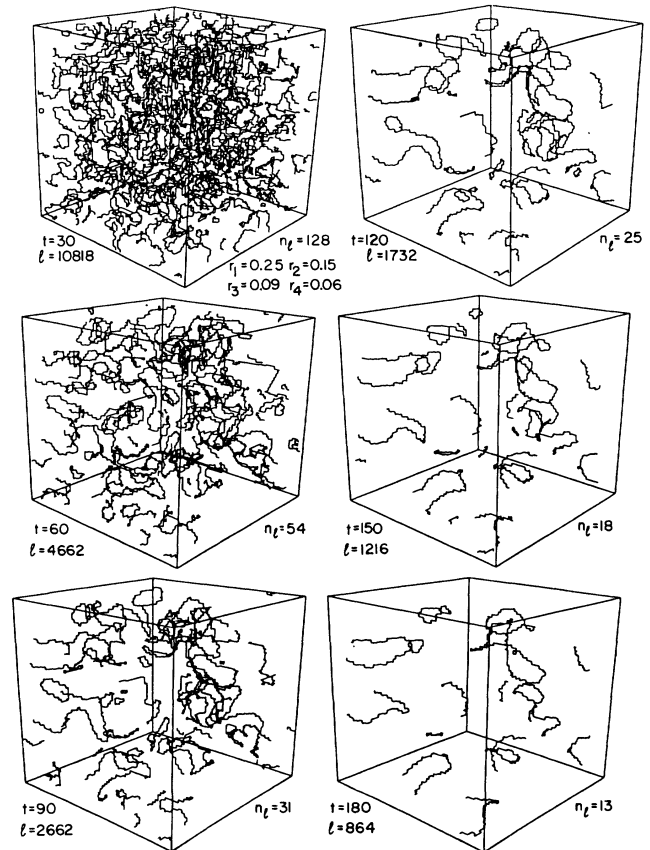

FIG. 2. Evolution of the string network after an off-critical quench ($|b|=0.001$). The bias is superimposed to the same initial condition used in Fig. 1 and the same conventions for the symbols apply.
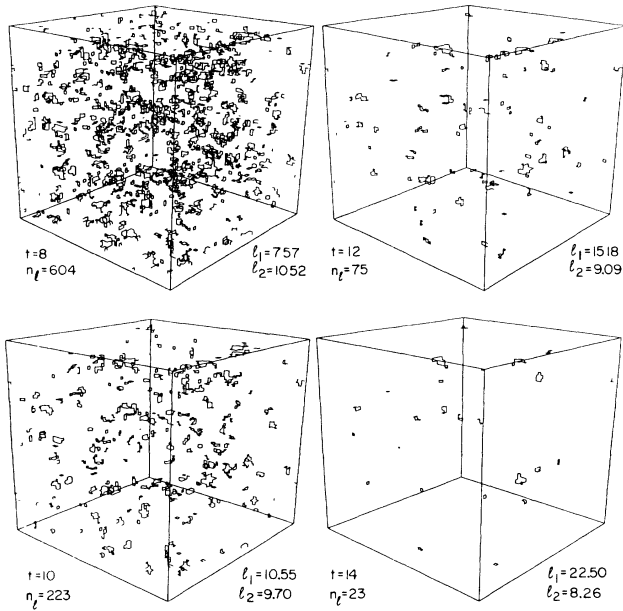
FIG. 3. Evolution of the string network after a strongly biased (off-critical) quench ($|b|=0.01$). The bias is superimposed to the same initial condition used in Fig. 1. Together with the number of loops $[n_l(t)]$ here we give the average inter-loop spacing $l_1(t) \equiv \sqrt{L^3/n_l(t)}$, where L is the size of the system, and the average loop size $l_2(t) \equiv l(t)/n_l(t)$, where $l(t)$ is the total string length.

FIG. 4. The graphs of $\log_{10}\lambda_m$, $m=1$ ($\circ$), 2 ($\triangle$), 3 ($\square$), $\log_{10}d$ (∇) and $\log_{10}r_{1/2}$ ($\Diamond$) vs $\log_{10}(t)$. The data were taken on 128^3 lattices and averaged over 40 initial conditions. Statistical fluctuations are shown whenever larger than the symbol size.

al shrinking and unwinding of this defect-string network. In our simulations we use periodic boundary conditions so that the defect network is a collection of closed oriented loops [22], possibly self-intersecting [23]. In fact, as shown in Fig. 1, the largest connected component of the network accounts for about three-quarters of the total string length $l(t)$ at early times, while the second largest loop is over one order of magnitude shorter. At later times we see the progressive opening of the network, clearly showing the reduction of the local string curvature.

For the off-critical case, the initial values of $X(\mathbf{r},0)$ and $Y(\mathbf{r},0)$ are randomly chosen to be between $-0.1 \pm |b|$ and $0.1 \pm |b|$, with $|b|=0.001$, $0.001/\sqrt{2}$, and $0.001/2$, so that $|\langle X(\mathbf{r},0)\rangle| = |\langle Y(\mathbf{r},0)\rangle| = |b|$. In this case we observe an early breakup of the string network and the subsequent decay of independent loops. For $|b|=0.001$, as seen in Fig. 2, we find that the number of small loops at early times has more than doubled with respect to the unbiased case, but the network still retains a number of significantly larger components that together account for about one-half of the total string length. Finally, if we choose $|b|=0.01$, the string network is completely destroyed (Fig. 3).

III. DYNAMICS AND POWER-LAW BEHAVIOR

We now turn to a detailed discussion of the dynamics. There are several, a priori independent, characteristic length scales in the system. The first three moments ($\overline{k}_1$,
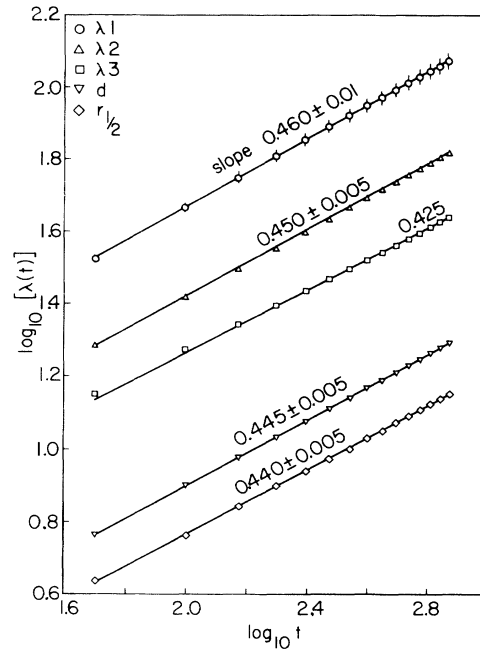
$\overline{k}_2$, and $\overline{k}_3$) of $S(k,t)$, the spherically averaged time-dependent scattering function [24],

$$\overline{k}_m(t) = \frac{\int_0^\infty dk\, k^m S(k,t)}{\int_0^\infty dk\, k^{m-1} S(k,t)}, \quad m=1,2,3 \qquad (3.1)$$

define three characteristic length scales, which we shall generically denote $\lambda_m(t) = L/[2\pi\overline{k}_m(t)]$, $m=1,2,3$. Alternatively, we can use the average interstring spacing defined as $d(t) = \sqrt{L^3/l(t)}$, where $l(t)$ is the total length of the vortex strings remaining at time t. There is also a characteristic length associated with the real-space correlation function of the order parameter

$$C(r,t) \equiv \frac{\langle \Psi^*(r,t)\Psi(0,t)\rangle}{\langle \Psi^*(0,t)\Psi(0,t)\rangle},$$

namely the half-width of the main peak of the correlation function $r_{1/2}(t)$, defined by the relation $C(r_{1/2}(t),t) = \frac{1}{2}$. The results are summarized in Fig. 4. In the time range investigated (50 to 750 time steps) the growth of four of the length scales considered [$\lambda_1(t)$, $\lambda_2(t)$, $d(t)$, and $r_{1/2}(t)$] can be well described by a single power law $\sim t^\phi$ with an effective exponent $\phi=0.45\pm0.01$, even though the growth might be slightly faster for the longer length scales and at later times. If there are any finite-size effects, then they should be within the limit of the quoted statistical uncertainty since, by the time we stop the simulation, $\lambda_1(750) \approx L$ but $d(750) \approx L/6$. In this time range $\lambda_3(t)$ shows a somewhat slower increase and there is also a statistically significant slope change

($\phi=0.4-0.425$). We conclude that the discrepancy with the mean-field result $\phi=0.5$ is not due to finite-size effects, but it is still possible that we have not yet reached the asymptotic regime [25]. In order to check this, longer simulations on even larger lattices would be necessary.

IV. CRITICAL QUENCH

As shown in Fig. 5, we find good evidence of dynamical scaling for the scattering function $S(k,t)=[\lambda(t)]^D\Phi(k\lambda(t))$, using $\lambda_1(t)$ as the rescaling length. We also find that, for $z\equiv k\lambda_1(t)>1$, the universal function decays as $\Phi(z)\sim z^\chi$, with $\chi=5.5\pm0.3$ (see inset of Fig. 5). As in the two-dimensional case [5] this power law reflects the single-vortex field configuration, which extends around each defect line up to distances comparable with the average interstring spacing $d(t)$ [26]. In Fig. 6 we show the scaling results for the real-space correlation function of the order parameter $C(r,t)$, where we have used $r_{1/2}(t)$ as the rescaling length. The small $x\equiv r/r_{1/2}(t)$ behavior of the universal function $C(r,t)=\Gamma(x)$ is shown in the inset of Fig. 6. We find
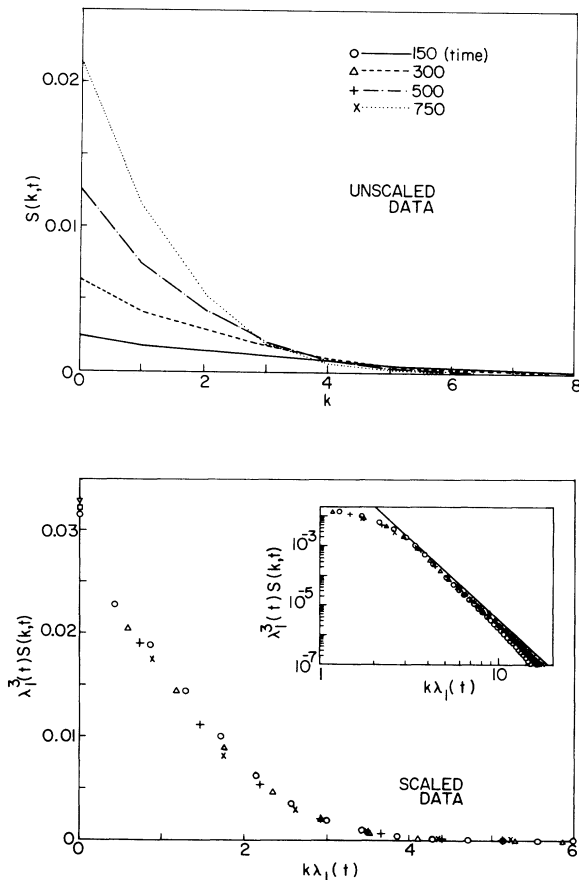
$\Gamma(x)\sim 1-x^\psi$, with $\psi=1.57\pm0.05$. This result coincides, within numerical uncertainties, with the result obtained in two dimensions [5] and shows that Porod's law (asymptotically valid for scalar systems) does not apply to systems with a continuous symmetry.

As for the vortex-vortex correlation functions in two dimensions [5] we find simple scaling also for the spherically averaged string-string correlation function $C_{SS}(r,t)$, as exhibited in Fig. 7. Up to distances comparable with $d(t)$ (or the average string curvature) the main contribution to the correlation function comes from points lying on the same branch of the network as the chosen reference point. This means that, at distances shorter than $d(t)$, but still larger than the vortex-core size ξ, the two-point correlation function simply reflects the connectivity of the network, and therefore, for $\xi/d(t)<y\equiv r/d(t)\ll 1$, $[d(t)]^{-2}C_{SS}(r,t)=\Gamma_{SS}(y)\sim y^{-2}$ (see inset of Fig. 7) [27]. On the other hand, for $r\gg d(t)$, we find, as expected, $C_{SS}(r,t)\sim[d(t)]^{-2}=l(t)/L^3$, the average string density in the system.

FIG. 5. Demonstration of dynamical scaling for the rescaled scattering function $\lambda_1(t)^{-3}S(k,t)=\Phi(k\lambda_1(t))$. We plot data taken at 150 (solid line, O) 300 (dashed line, $\triangle$), 500 (chain dotted line, $+$), and 750 (dotted line, $\times$) time steps (averaged over 40 initial conditions). Inset shows a log-log plot of the universal function and, for comparison, a solid line with a slope of -5.5.
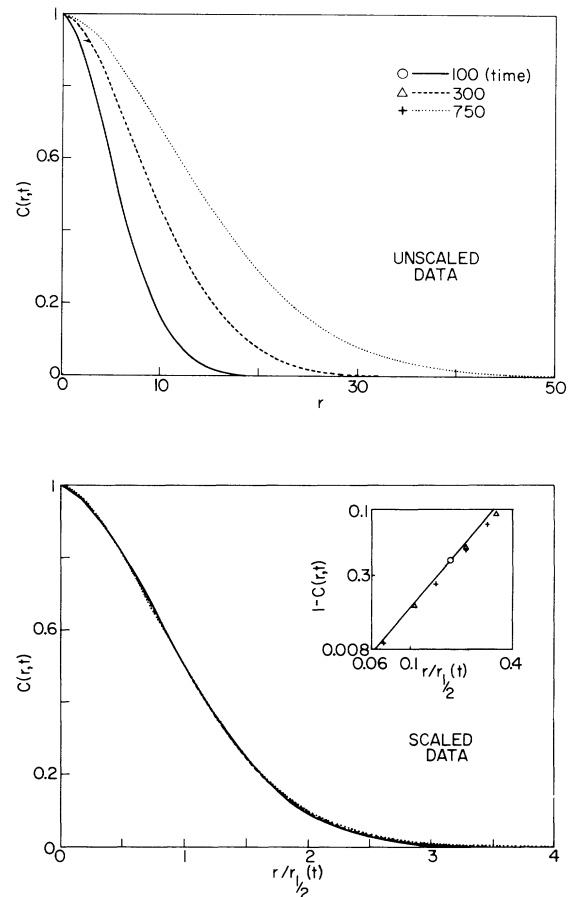

FIG. 6. Demonstration of dynamical scaling for the real-space correlation function of the order parameter $C(r,t)=\Gamma(r/r_{1/2}(t))$, where $r_{1/2}(t)$ is the half-width of $C(r,t)$. We plot data taken at 100 (solid line, O), 300 (dashed line, $\triangle$), and 750 (dotted line, $+$) time steps. We averaged over 40 initial conditions. Inset shows a log-log plot of $1-\Gamma(x)$ in the limit of small x and, for comparison, a solid line with a slope of 1.57.
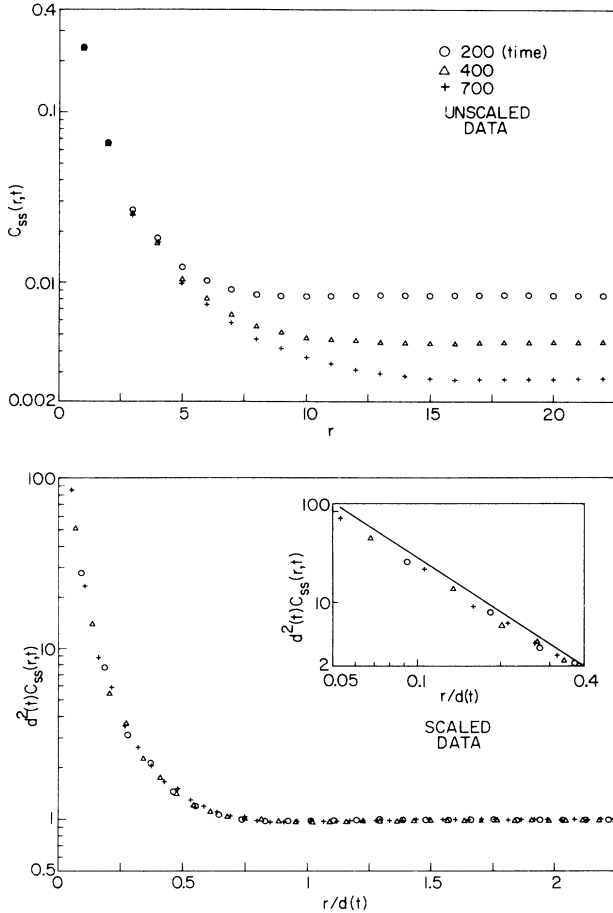
FIG. 7. Demonstration of dynamical scaling for the real-space string-string correlation function $C_{SS}(r,t)$ $=d(t)^{-2}\Gamma_{SS}[r/d(t)]$, where $d(t)$ is the average interstring spacing. The data were taken at 200 ($\bigcirc$), 400 ($\triangle$), and 700 (+) time steps (averaged over 10 initial conditions). Inset shows a log-log plot of $\Gamma_{SS}(x)$ in the limit of small x and, for comparison, a solid line with a slope of -2.

Note that, as mentioned above, the natural rescaling length for the string-string correlation function at short distances is the average local curvature of the string. The existence of scaling implies that the average values of the local curvature and interstring spacing have the same time dependence. Note also that, as seen in Fig. 7, the narrow transition region $[r \sim d(t)]$ is characterized by a slight dip in the correlation function.

V. OFF-CRITICAL QUENCH

We have performed three series of simulations using different values of $|\langle \Psi(r,0) \rangle| = \sqrt{2}|b| > 0$ in order to check the exponential decay law for the total string length $l(t) \sim t^{-1}\exp(-\gamma t^{3/2})$ and the relation $\gamma \propto |b|^2$. The results are shown in Fig. 8. We find good quantitative agreement with the value of $\frac{3}{2}$ for the exponent. We also find that γ grows somewhat faster than quadratically with increasing $|b|$. A similar discrepancy with the theory was found in the scalar case [17]. From Fig. 8 we can see that not only the strength, but also the onset time
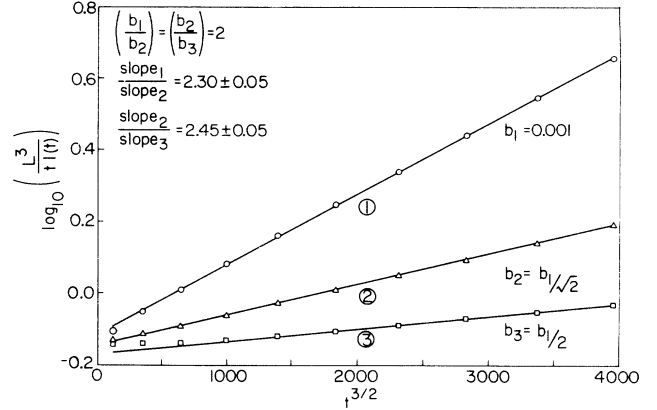

FIG. 8. Graph of $\log_{10}[L^3/tl(t)]$ versus $t^{3/2}$ for $|b| = 0.001$ ($\bigcirc$), $0.001/\sqrt{2}$ ($\triangle$), and $0.001/2$ ($\square$). We obtained our statistical ensembles by superimposing each value of the bias ($|b|$) over the same 30 random initial conditions.

(t_c) of the exponential decay is controlled by the magnitude of $|b|$. In fact, even in the $b = 0$ case, the spatial average of the initial field configuration over any finite volume (l^3) of the system shows statistical fluctuations $|\langle \Psi(r,0) \rangle||_{|b|=0} \sim \sigma_0(a/l)^{3/2}$, where σ_0 is the standard deviation of the order parameter at each site and a is the lattice spacing. If we now make the natural assumption that the crossover is controlled by the ratio of $|b|$ versus the amplitude of these statistical fluctuations, we can introduce a crossover length $l_c(b) \sim a(\sigma_0/|b|)^{2/3}$ such that when the characteristic length scale in the system $\lambda(t_c) \sim l_c(b)$, the relaxation process changes from a power law to an exponential decay [28].

In Fig. 3 we show the evolution of the system for $|b| = 0.01$. In this case we observe a complete breakup of the string network after only a few time steps $[l_c(0.01) \sim 3a]$ followed by the shrinking of independent vortex loops. The widely spaced loops that remain at the end of the sequence are the few larger-than-average loops found at the beginning of the sequence. Considerations similar to the ones introduced in the previous paragraph suggest that, after the breakup of the network, the probability of finding a loop of radius $r > l_c(b)$ will decrease with increasing r as $\exp[-\gamma_0(r/a)^3]$, where $\gamma_0 \propto (|b|/\sigma_0)^2$. The radius of each individual loop will then decay in a finite time [we expect $r(t) \sim \sqrt{r(0)^2 - D_f t}$ for a circular loop of initial radius $r(0)$ and an effective diffusion constant D_f] so that the exponential decay of the total length of the string network $l(t)$ will depend on the initial size distribution of the loops [29]. In order to characterize the ordering process we now need at least two length scales: the average size of vortex loops, which have only a weak time dependence [30], and the average interloop spacing, which increases exponentially with time due to the annihilation of the smaller loops. Figure 3 shows that at late times the size of the remaining loops is slowly decreasing, whereas the distance between them rapidly increases with time. Thus, the very existence of two length scales with widely different time dependencies clearly indicates the complete

breakdown of dynamical scale invariance. At this stage, however, we cannot rule out the possibility that there may be a complicated crossover scaling involving the bias strength, which if it exists, would represent an extension of the usual notion of scaling in these systems. This possibility will be investigated in future studies.

VI. DISCUSSION

We have presented the results of a numerical study of the coarsening dynamics of a three-dimensional system with a nonconserved complex order parameter $\Psi(\mathbf{r},t)$. We have found that the ordering dynamics depends on the initial value of the spatial average of the order parameter $[\langle \Psi(\mathbf{r},0)\rangle = \sqrt{2}b]$ after the quench below the ordering transition temperature. For the critical quench ($b=0$), we observe dynamical scaling and an effective value of the dynamical exponent of $\phi=0.45\pm0.01$. For the off-critical quench ($|b|>0$), dynamical scaling breaks down, and the decay of the vortex-string length $l(t)$ becomes exponential $l(t)\sim t^{-1}\exp(-\gamma t^{3/2})$. The relation $\gamma \propto |b|^2$, predicted by Toyoki and Honda [9], appears to be in fact a lower bound. We stress that the dynamics of the string is controlled in both cases by the tension corresponding to its local curvature. The sharply different time dependence in the two regimes is due to the essential difference in the global connectivity of the network after the quench.

These results reflect rather general properties of the relaxation process for systems with a nonconserved order parameter. For example, if we repeat the calculation of Toyoki and Honda [9] in the case of a two-dimensional system (where the vortex strings reduce to vortex points), we find that the average number of vortices in the system $N_v(t)$ should decay as $N_v(t)\sim t^{-1}\exp(-\gamma t)$, with $\gamma \geq 0$ ($\gamma=0$ corresponds to the critical quench) [31]. We can also extend this approach to a system with a Heisenberg order parameter $\Sigma(\mathbf{r},t)=(X(\mathbf{r},t),Y(\mathbf{r},t),Z(\mathbf{r},t))$ in three dimensions. The topologically stable defects in this case

are point defects (hedgehogs). We can describe them as intersections of three surfaces representing the zeros of three auxiliary scalar fields. Identifying these fields with the three components of the order parameter, we again predict [32] that the number of point defects $N_{\mathrm{PD}}(t)$ will decrease with time as $N_{\mathrm{PD}}(t)\sim t^{-3/2}\exp(-\gamma t^{3/2})$, where $\gamma \propto |\langle \Sigma(\mathbf{r},0)\rangle|^2$. These considerations might be of relevance to cosmological pattern formation, since they indicate that the final distribution of topological defects, following a phase transition characterized by a nonconserved order parameter, is extremely sensitive to the initial conditions.

After the submission of this work for publication, Toyoki pointed out to us that, in a more recent paper, Nagaya, Orihara, and Ishibashi [33] also recognized that their experiment was a realization of the situation discussed by Toyoki and Honda [17]; furthermore, their measurements of the decay of the total length of disclination lines are consistent with theoretical predictions. Note that these experiments are effectively performed with a constant external field, rather than simply a bias in the initial condition. The fact that the results in this situation agree with the calculation is consistent with our expectations as explained in the Introduction of this paper.

[1] General overviews of the field can be found in H. Furukawa, Adv. Phys. **34**, 703 (1985); J. D. Gunton, M. San Miguel, and P. S. Sahni, in *Phase Transitions and Critical Phenomena*, edited by C. Domb and J. L. Lebowitz (Academic, New York, 1983), Vol. 8.

[2] B. D. Gaulin, S. Spooner, and Y. Morii, Phys. Rev. Lett. **59**, 668 (1987); R. Toral, A. Chakrabarti, and J. D. Gunton, *ibid.* **60**, 2311 (1988).

[3] K. Kawasaki and T. Ohta, Physica A **118**, 175 (1983), and references therein.

[4] A. J. Bray and K. Humayun, J. Phys. A **23**, 5897 (1990); A. J. Bray, Phys. Rev. B **41**, 6724 (1990).

[5] M. Mondello and Nigel Goldenfeld, Phys. Rev. A **42**, 5865 (1990). For a related simulation of the quenched dynamics of the *XY* model, see R. Loft and T. A. DeGrand, Phys. Rev. B **35**, 8528 (1987).

[6] Fong Liu, M. Mondello, and Nigel Goldenfeld, Phys. Rev. Lett. **66**, 3071 (1991).

[7] H. Nishimori and T. Nukii, J. Phys. Soc. Jpn. **58**, 563 (1989).

[8] H. Toyoki, J. Phys. Soc. Jpn. **60**, 1433 (1991).

[9] H. Toyoki and K. Honda, Prog. Theor. Phys. **78**, 273 (1987).

[10] K. Kawasaki, Phys. Rev. A **31**, 3880 (1985), and references therein.

[11] This is an extension to a system with vector order parameter of the random-interface dynamics originally introduced by T. Otha, D. Jasnow, and K. Kawasaki, Phys. Rev. Lett. **49**, 1223 (1982), to study the ordering process in the scalar case.

[12] See M. Mondello and Nigel Goldenfeld, Ref. [5], footnote 21.

[13] I. Chuang, N. Turok, and B. Yurke, Science **251**, 1336 (1991).

[14] H. Orihara and Y. Ishibashi, J. Phys. Soc. Jpn. **55**, 2151 (1986).

[15] T. Nagaya, H. Orihara, and Y. Ishibashi, J. Phys. Soc. Jpn. **56**, 3086 (1987).

[16] A discussion of the topological classification of defects in liquid crystals is given in L. Michel, Rev. Mod. Phys. **52**, 617 (1980). A less mathematical introduction to defects and textures in nematics can be found, for example, in

P. G. de Gennes, *The Physics of Liquid Crystals* (Clarendon, Oxford, 1974).

[17] H. Toyoki and K. Honda, Phys. Rev. B **33**, 385 (1986).

[18] The equation of motion proposed in Ref. [15] for disclination lines in nonorthogonally twisted nematics is $R = -\Gamma/R - D\epsilon$, where R is the local radius of curvature, $\epsilon(=\pi/2-\theta)$ is the deviation from orthogonal twisting, and Γ and D are positive constants. Using this equation and assuming that the bias is applied only during the late stages of the coarsening dynamics, we would expect a crossover from $R \sim t^{-1/2}$, valid for $\epsilon=0$, to $R \sim t^{-1}$, valid for $\epsilon > 0$ and $R \gg \Gamma/D\epsilon$. In contrast, when the bias is applied during the quench, we expect an exponential decay.

[19] Strictly speaking one should compare the "effective" size L/ξ of the two simulations, where L is the size of the system and ξ the static correlation length. An independent argument suggesting that finite-size corrections are not dominant in the time range considered is discussed in Sec. III.

[20] Y. Oono and S. Puri, Phys. Rev. Lett. **58**, 836 (1987); Phys. Rev. A **38**, 434 (1988); A. Chakrabarty and J Gunton, Phys. Rev. B **37**, 3798 (1988); Y. Oono and M. Bahiana, Phys. Rev. Lett. **61**, 1109 (1988).

[21] This is strictly true only for an infinite system or for a sample averaged over an infinite number of initial conditions. We will return to this issue in Sec. V.

[22] The loop orientation in a three-dimensional system corresponds to the vortex sign (charge) in a two-dimensional system. With periodic boundary conditions, we have closed loops in three dimensions and charge neutrality in two dimensions.

[23] We note that in our simulations the equilibrium correlation length (vortex-core radius) extends over roughly two lattice spacings. It is, therefore, natural to consider all intersections that occur in the network (that is, all cases of multiple strings entering and exiting the same lattice box) as self-intersections of the same string component (loop). With this restriction, there is only one way to decompose the network in mutually disconnected self-intersecting loops, and we have developed an algorithm to compute the corresponding loop-size distribution.

[24] All our measurements involve an ensemble averaging over initial conditions and, for space- or wave-vector-dependent quantities, an average over all directions. In the discrete spherical average, we chose k (r) to be the nearest integer to $|k|$ $(|r|)$.

[25] In this regard we note that in our two-dimensional simulations, a long transient was observed during the first 1500 updates, see M. Mondello and Nigel Goldenfeld, Ref. [5]. See also the final comment in the Introduction of this paper.

[26] The spherical average of the scattering function of a cylindrically symmetric vortex-field configuration is $\sim k^{-5}$. We would expect this power law to be satisfied for wavelengths λ ($=2\pi/k$) in the range $\xi < \lambda < \lambda_s$, where ξ is the vortex-core size and λ_s is the shortest length among the average interstring distance $[d(t)]$, the average (local) radius of curvature of the string and the characteristic length for "torsional" deformation of the vortex field.

[27] This singular behavior simply reflects the fact that we are considering a *point* correlation function of an *extended* defect, and the behavior represents a true singularity, of course, only in the case of an infinitely thin string. In our numerical calculation, the lattice spacing provides the most convenient cutoff, although in reality, the only natural cutoff is represented by the vortex-core size.

[28] In the preceding analysis we have implicitly assumed that $|b| \gg \sigma_0(a/L)^{3/2}$, where L is the size of the system. In the limit $|b| \to 0$ (critical quench) $\sigma_0(a/L)^{3/2}$ becomes the dominant contribution to $|\langle \Psi(r,0)\rangle|_{|b|\to 0}$ and $l_c(0) \sim L$; that is, the crossover will never occur.

[29] This discussion makes explicit the physical content of the (biased) initial conditions adopted by Toyoki and Honda in Ref. [9]. It also suggests that the precise $\gamma(b)$ dependence parametrizes the dynamical information of the early breakup phase and is therefore beyond the scope of a mean-field treatment.

[30] This time dependence is determined by two competing factors: the decrease in size of the individual loops and the progressive disappearance (elimination from the average) of the smaller ones.

[31] Note that we could rewrite the $D=2$ and the $D=3$ results as $l_D(t) \sim t^{-1}\exp(-\gamma_D t^{D/2})$. An analogous relation is found in the scalar order-parameter case. See H. Toyoki and K. Honda, Ref. [17].

[32] The power-law decay for the number of point defects after a critical quench has been confirmed in a recent numerical study by H. Toyoki, J. Phys. Soc. Jpn. **60**, 1153 (1991).

[33] T. Nagaya, H. Orihara, and Y. Ishibashi, J. Phys. Soc. Jpn. **59**, 377 (1990).